

## The Crystal Structure of High ( $\gamma$ )-Li<sub>2</sub>BeSiO<sub>4</sub>: a Tetrahedral Structure

BY R. A. HOWIE AND A. R. WEST

University of Aberdeen, Department of Chemistry, Meston Walk, Aberdeen AB9 2UE, Scotland

(Received 16 October 1973; accepted 15 July 1974)

The crystal structure of high ( $\gamma$ )-Li<sub>2</sub>BeSiO<sub>4</sub> has been solved from three-dimensional single-crystal X-ray diffraction data ( $R=4.7\%$ ). It is directly related to the structures of LiAlO<sub>2</sub>, NaAlO<sub>2</sub> and NaFeO<sub>2</sub> ( $\gamma$ , high forms). The orthorhombic symmetry and cell of  $\gamma$ -Li<sub>2</sub>BeSiO<sub>4</sub>,  $a=6.853$ ,  $b=6.927$ ,  $c=6.125$  Å, space group  $C222_1$ , as distinct from the tetragonal symmetry of  $\gamma$ -LiAlO<sub>2</sub> *etc.*, is due to systematic, ordered, replacement of aluminum or iron(III) by silicon and beryllium. The oxygen atoms form a distorted hexagonal close-packed arrangement; the cations are distributed over half the available tetrahedral sites on either side of the oxygen layers. Mean bond distances for Si-O and Be-O are 1.635 and 1.647 Å respectively. Variations in Li-O bond distances are discussed.

### Introduction

The crystal structure of high ( $\gamma$ )-Li<sub>2</sub>BeSiO<sub>4</sub> is part of a program of investigation of oxides of the general formula  $A_2^+B^{2+}X^{4+}O_4$ . The interest in the structure lies in evaluating the nature of the relationship between this structure and that of the tetragonal oxides  $\gamma$ -LiAlO<sub>2</sub>,  $\gamma$ -NaAlO<sub>2</sub> and  $\gamma$ -NaFeO<sub>2</sub>.

### Experimental

#### Growth of single crystals

Single crystals of  $\gamma$ -lithium beryllium orthosilicate were selected from a melt of approximate composition Li<sub>2</sub>BeSiO<sub>4</sub> which had been cooled from 1500 to 1100 °C over a period of 24 hr and then quenched to room temperature.

#### Crystal data

$\gamma$ -Li<sub>2</sub>BeSiO<sub>4</sub> forms platy crystals of moderately low birefringence with cleavage (001). In the cleavage plane, refractive indices vary from  $1.608 \pm 0.004$  to  $1.618 \pm 0.004$  and the extinction directions are at 45° to crystallographic **a** and **b**. The crystal system is orthorhombic,  $a=6.853 \pm 0.009$ ,  $b=6.927 \pm 0.009$ ,  $c=6.125 \pm 0.008$  (refined from powder-diffraction data\*), space group  $C222_1$  (absent reflexions  $hkl$  with  $h+k$  odd and  $00l$  with  $l$  odd, from rotation, oscillation and Weissenberg photographs about [110] and  $c$ ),  $Z=4$ , Li<sub>2</sub>BeSiO<sub>4</sub>, F.W. 115.07,  $D_{calc}=2.629$ ,  $D_{obs}=2.56$  g cm<sup>-3</sup> (displacement of air).

#### Intensity data collection

Because of the close similarity of the orthorhombic cell edges  $a$  and  $b$ , it was possible, for the purposes of data collection only, to re-index the *measured* reflex-

ions on a primitive orthogonal cell:  $a'=r/\sqrt{2}$  coincident with [1 $\bar{1}$ 0],  $b'=r/\sqrt{2}$  coincident with [110], where  $r=(a+b)/2$ , and  $c'$  equal to and coincident with  $c$ . The data were collected, with the crystal (approximately 0.5 × 0.5 × 0.1 mm) rotating about **b'**, on a Hilger and Watts Y-190 linear diffractometer with Mo  $K\alpha$  radiation. The angle of scan ( $\omega$ ) of the diffractometer was 1.3° and the time for each measurement cycle was one minute, apportioned equally between two background counts – one on either side of the Bragg angle (crystal stationary) – and scan motion through the Bragg angle. The balanced filter facility of the diffractometer was employed and eight measurement cycles, which reduce to four estimates of the net intensity, were made on each reflexion. No absorption correction was applied.

#### Intensity reduction

Initially, the intensities of the two classes of reflexion  $h'k'l$  and  $h'k'\bar{l}$  ( $k \neq 0$ ), and  $h'0l$ ,  $\bar{h}'0l$ ,  $h'0\bar{l}$  and  $\bar{h}'0\bar{l}$  were averaged and  $L_p$  factors applied.\* Layer scale factors were obtained ranging from 1.00 to 1.297, by comparison of the  $h'0l$  and  $0h'l$  structure amplitudes. In a second pass, the layer scale factors (on  $k'$ ) were applied, and the data re-indexed by the transformation  $110/\bar{1}10/001$ . The reflexions  $hkl$ ,  $h\bar{k}l$ ,  $\bar{h}kl$  and  $\bar{h}\bar{k}l$  were averaged to yield 317 independent structure amplitudes on an arbitrary scale, of which 14 reflexions were classed as unobserved, as their original intensities were less than three times the corresponding standard deviation, based on counting statistics.

### Programs

The programs used in the refinement were those of Ahmed & Barnes of the National Research Council of Canada, adapted for use with the ICL4-50 computer by J. S. Knowles of the Computing Department of the University of Aberdeen. Least-squares refinement employed the block-diagonal approximation and the weighting scheme used throughout was  $1/w=|F_o|/K$ ,

\* The indexed X-ray powder diffraction data and table of observed and calculated structure factors have been deposited with the British Library Lending Division as Supplementary Publication No. SUP 30582 (5 pp.). Copies may be obtained through The Executive Secretary, International Union of Crystallography, 13 White Friars, Chester CH1 1NZ, England.

\* Primes indicate indices referred to the pseudocell.

( $|F_o| \leq K$ ) or  $|w = K/|F_o|$ , ( $F_o > K$ ) where  $K$  was set to 10.0 on the absolute scale. Atomic scattering factors were taken from *International Tables for X-ray Crystallography* (1968). Anomalous dispersion was not considered. The anisotropic temperature factors in this program are of the form  $\exp[-(B_{11}h^2 + B_{22}k^2 + B_{33}l^2 + B_{23}kl + B_{13}hl + B_{12}hk)]$ . The standard deviations of the refined parameters are given by  $[A_{ii}^{-1} \times \sum W\Delta F^2 / (m - n)]^{1/2}$ , where  $A_{ii}^{-1}$  is the diagonal element of the inverse normal equations matrix corresponding to the  $i$ th parameter,  $m$  is the number of independent reflexions (observations) and  $n$  is the number of parameters refined.

### Solution of the structure

A Patterson map, constructed from the squares of the

observed structure amplitudes, yielded the positions of the silicon atoms unambiguously. Oxygen atom positions were also obtained, but these were related by pseudo-symmetry, arising from overlap of vectors, which was destroyed by placing one of the lithium atoms in a position estimated from comparison of the pseudo-symmetric structure with that of  $\gamma$ -LiAlO<sub>2</sub> (Marezio, 1965; Bertaut, Delapalme, Bassi, Durif-Varambon & Joubert, 1965). Least-squares refinement (five cycles) produced improved coordinates for oxygen and silicon [ $R = 32\%$ , where  $R = 100 \times (\sum |F_{\text{obs}} - F_{\text{calc}}| / \sum |F_{\text{obs}}|) \%$ ].

From consideration of bond lengths and angles, it was apparent that the original lithium atom was wrongly placed. However, its true position as well as that of the remaining lithium and beryllium atoms was

Table 1. Atomic parameters for high Li<sub>2</sub>BeSiO<sub>4</sub>

Estimated standard deviations are in parentheses.  $B_{ij}$  are  $\times 10^4$ .

	$N^a$	$x$	$y$	$z$	$B_{\text{iso}}^b$	$B_{11}$	$B_{22}$	$B_{33}$	$B_{23}$	$B_{13}$	$B_{12}$
O(1)	8(c)	-0.0315 (2)	0.3140 (2)	0.0339 (2)	0.59 (3)	41 (2)	31 (2)	30 (4)	18 (4)	2 (4)	18 (4)
O(2)	8(c)	0.1877 (2)	0.0356 (2)	0.2192 (2)	0.66 (3)	35 (2)	39 (2)	36 (3)	-4 (4)	19 (4)	29 (4)
Si	4(b)	0.0000	0.1805 (1)	0.2500	0.41 (1)	27 (1)	23 (1)	20 (2)		4 (2)	
Li(1)	4(a)	0.1833 (9)	0.5000	0.0000	1.05 (7)						
Be	4(a)	0.1813 (5)	0.5000	0.5000	0.59 (4)						
Li(2)	4(b)	0.0000	0.7990 (9)	0.2500	1.47 (8)						

(a) Number of positions and Wyckoff notation. (b) Units of  $B_{\text{iso}}$  are  $\text{\AA}^2$ .

Table 2. Representative bond distances ( $\text{\AA}$ ) and angles ( $^\circ$ ) for high Li<sub>2</sub>BeSiO<sub>4</sub>

<b>SiO<sub>4</sub></b>		<b>Li(1)O<sub>4</sub></b>	
Si—O(1)	1.629 (2)	Li—O(1)	1.967 (5)
Si—O(2)	1.642 (2)	Li—O(2')	1.950 (3)
O(1)—O(1')	2.682 (2)	O(1)—O(1'')	2.611 (2)
O(2)—O(2')	2.600 (2)	O(2')—O(2''')	3.475 (2)
O(1)—O(2)	2.695 (2)	O(1)—O(2')	3.218 (2)
O(1)—O(2')	2.674 (2)	O(1)—O(2'')	3.193 (2)
O(1)—Si—O(1')	110.84 (7)	O(1)—Li—O(1'')	83.13 (14)
O(2)—Si—O(2')	104.65 (7)	O(2')—Li—O(2''')	126.07 (19)
O(1)—Si—O(2)	110.93 (7)	O(1)—Li—O(2')	110.47 (17)
O(1)—Si—O(2')	109.66 (7)	O(1)—Li—O(2'')	109.20 (17)
<b>Li(2)O<sub>4</sub></b>		<b>BeO<sub>4</sub></b>	
Li—O(1'')	1.919 (3)	Be—O(1')	1.660 (3)
Li—O(2')	2.092 (5)	Be—O(2')	1.634 (3)
O(1'')—O(1''')	3.505 (2)	O(1')—O(1''')	2.611 (2)
O(2')—O(2)	2.600 (2)	O(2')—O(2''')	2.730 (2)
O(1'')—O(2')	3.244 (2)	O(1')—O(2')	2.711 (2)
O(1'')—O(2)	3.275 (2)	O(1')—O(2''')	2.682 (2)
O(1'')—Li—O(1''')	131.89 (21)	O(1')—Be—O(1''')	103.66 (13)
O(2')—Li—O(2)	76.84 (14)	O(2')—Be—O(2''')	113.31 (14)
O(1'')—Li—O(2')	107.86 (18)	O(1')—Be—O(2')	110.73 (14)
O(1'')—Li—O(2)	109.39 (18)	O(1')—Be—O(2''')	108.99 (14)
<b>O(1)SiBeLi<sub>2</sub></b>		<b>O(2)SiBeLi<sub>2</sub></b>	
Si—Li(2)	3.066 (0)	Si—Li(2)	2.643 (6)
Si—Li(1)	2.970 (3)	Si—Li(1)	2.936 (4)
Si—Be	2.964 (2)	Si—Be	2.946 (3)
Li(2)—Be	2.859 (5)	Li(2)—Li(1)	2.999 (5)
Li(2)—Li(1)	2.866 (5)	Li(2)—Be	3.009 (4)
Be—Li(1)	2.498 (7)	Li(1)—Be	3.063 (0)
Si—O—Be	128.62 (11)	Si—O—Be	128.10 (12)
Si—O—Li(2)	119.35 (13)	Si—O—Li(2)	89.25 (12)
Si—O—Li(1)	111.00 (12)	Si—O—Li(1)	109.33 (13)
Li(1)—O—Li(2)	95.00 (16)	Li(1)—O—Li(2)	95.74 (15)
Li(1)—O—Be	86.61 (14)	Li(1)—O—Be	117.17 (15)
Li(2)—O—Be	105.81 (15)	Li(2)—O—Be	107.09 (14)

easily derived from the positions of the oxygen atoms. Ten further least-squares cycles, allowing the atoms to vibrate isotropically, reduced  $R$  to 4.99%. Refinement was continued for four cycles with anisotropic temperature factors applied to the silicon and oxygen atoms and isotropic factors applied to the remainder. Unobserved data, and 24 other reflexions for which  $\Delta F/F > 0.12$ , were excluded and the final  $R$  over 279 reflexions was 2.88%. This final solution corresponds to an  $R$  over all data of 4.7%. At this stage, a difference map showed no peaks larger than  $0.8 \text{ e } \text{\AA}^{-3}$  (1% of the Si peak and 10% of a lithium peak), whereas the Fourier (electron density) map showed the atoms in the expected positions with appropriate electron densities. The distribution of weighted residuals ( $\sum W\Delta F^2$ ) both in terms of  $\sin^2 \theta$  and  $|F_o|$  (excepting a few of the strongest reflexions which showed poor agreement with the calculated values owing to extinction) suggested that the weighting scheme used was satisfactory. The final atomic coordinates and bond lengths and angles are given in Tables 1 and 2 respectively. A (001) projection of the structure is shown in Fig. 1, together with representative bond distances.

### Description of the structure

The crystal structure of high ( $\gamma$ )-Li<sub>2</sub>BeSiO<sub>4</sub> is directly related to that of the high-temperature,  $\gamma$ -polymorphs of LiAlO<sub>2</sub>, NaAlO<sub>2</sub> and NaFeO<sub>2</sub>. The relation between  $\gamma$ -LiAlO<sub>2</sub> and  $\gamma$ -LiBeSiO<sub>4</sub> is simply:  $2\text{Al}^{3+} \rightleftharpoons \text{Be}^{2+} + \text{Si}^{4+}$ . Ordering of the beryllium and silicon atoms on

the aluminum sites lowers the symmetry from tetragonal  $P4_22_1$  to orthorhombic  $C22_1$ .  $\gamma$ -Li<sub>2</sub>BeSiO<sub>4</sub> may be classified as a distorted stuffed cristobalite structure. The SiO<sub>4</sub> and BeO<sub>4</sub> tetrahedra are linked in a similar manner to the SiO<sub>4</sub> tetrahedra of cristobalite, but the Be-O-Si bond angles of  $128^\circ$  are considerably removed from the ideal  $180^\circ$ . Charge balance is preserved by stuffing lithium into available tetrahedral holes.

### Details of the structure and discussion

The oxygen atoms form an approximately hexagonal close-packed arrangement with some buckling of the individual oxygen layers: close-packed layers are seen perpendicular to both [110] and  $\bar{1}\bar{1}0$ . The cations occupy half the available tetrahedral sites and are distributed equally over the sites on either side of the oxygen layers. The distribution of cations is such that the tetrahedral sites between any two adjacent oxygen layers contain either Li(2) and Si atoms or Li(1) and Be atoms. The occupancy of the tetrahedral sites causes each cation to share two oxygens, *i.e.* a tetrahedron edge, with another cation of different kind. Thus, Li(2) and Si share two common O(2) oxygens while Li(1) and Be share two O(1) oxygens. This sharing of tetrahedron edges can be seen from Fig. 1. A schematic, distorted (001) projection of the structure is shown in Fig. 2. Differences in sizes of the various cation-oxygen tetrahedra (MO<sub>4</sub>) have been ignored, as have distortions of the tetrahedra and buckling of the oxygen layers. However, Fig. 2 does show the alternate layers

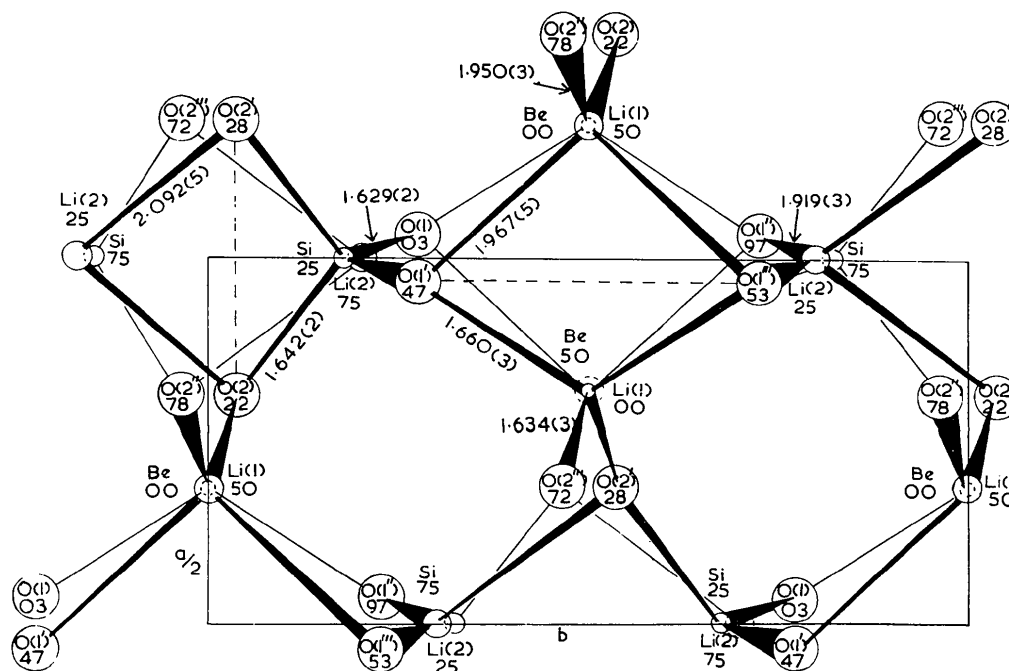


Fig. 1. (001) projection of  $\gamma$ -Li<sub>2</sub>BeSiO<sub>4</sub>. Smallest circles are Si or Be, intermediate Li and largest O.  $z$  coordinates, in units of  $c/100$ , are given as subscripts to the atom designations. The latter are the same as those used in the text. Dashed lines indicate common edges of MO<sub>4</sub> tetrahedron pairs.

of  $\text{Li}(2)\text{O}_4\text{-SiO}_4$  and  $\text{BeO}_4\text{-Li}(1)\text{O}_4$  tetrahedral pairs, packed along  $[110]$ . A similar sequence of layers of paired tetrahedra is encountered along  $[\bar{1}10]$ .

The orientation of the tetrahedron pairs, e.g. the  $\text{Li}(2)\text{O}_4\text{-SiO}_4$  pairs, is such that their common edge is parallel to  $\mathbf{a}$ , and pairs are stacked parallel to  $\mathbf{c}$  to form columns, or double chains. A schematic (100) projection of such a column is shown in Fig. 3. The two oxygen atoms constituting each shared edge have somewhat different  $c$  values, but this difference is ignored in Fig. 3. Neighbouring columns of  $\text{Li}(2)\text{O}_4\text{-SiO}_4$  tetrahedra are linked at their corners *via* columns constructed similarly from  $\text{Li}(1)\text{O}_4\text{-BeO}_4$  tetrahedral pairs to form a three-dimensional network of linked tetrahedra. The latter columns are oriented with their shared oxygen edges parallel to  $\mathbf{b}$ .

Each  $\text{MO}_4$  tetrahedron vertex, *i.e.* each oxygen atom, is shared with three other tetrahedra. Thus, the coordination of the oxygens as well as that of the cations is tetrahedral, and the structure is one of a family of so-called tetrahedral structures (Parthé, 1964). If, in fact, the structure is considered as built of oxygen-centred tetrahedra ( $\text{OM}_4$ ), instead of cation-centred tetrahedra, a similar network of linked tetrahedra arises. The shared edges are now found between pairs of adjacent  $\text{O}(1)\text{M}_4$  tetrahedra and between pairs of adjacent  $\text{O}(2)\text{M}_4$  tetrahedra.

The mean bond lengths in  $\gamma\text{-Li}_2\text{BeSiO}_4$  are:  $\text{Li}(1)\text{-O}$  1.959,  $\text{Li}(2)\text{-O}$  2.006,  $\text{Be-O}$  1.647 and  $\text{Si-O}$  1.635 Å. The average bond lengths for tetrahedral coordination given in *International Tables for X-ray Crystallography* (1968) are  $\text{Li-O}$  1.98,  $\text{Be-O}$  1.65,  $\text{Si-O}$  1.612 Å. How-

ever, all the tetrahedra in  $\gamma\text{-Li}_2\text{BeSiO}_4$  are distorted to varying degrees. The  $\text{O}(2)\text{-O}(2)$  edge common to the  $\text{Li}(2)$ -centred and  $\text{Si}$ -centred tetrahedra is 2.600 Å. This value is a little shorter than the average (2.684 Å) of the other five edges of the  $\text{SiO}_4$  tetrahedron but is much shorter than the average (3.309 Å) of the other five edges of the  $\text{Li}(2)\text{O}_4$  tetrahedron, and so the  $\text{Li}(2)\text{O}_4$  tetrahedron is grossly distorted. Because they occupy edge-sharing tetrahedra, the  $\text{Li}(2)$  and  $\text{Si}$  cations will repel one another strongly. Despite the screening effect of the short, shared, tetrahedron edge and the resultant increase in distance between the two cations of the tetrahedron pair, the cations are further displaced, off the centres of their tetrahedra, and away from the common edge. Thus, the bonds to the common oxygens [ $\text{Li-O}(2)$  2.092,  $\text{Si-O}(2)$  1.642 Å] are longer than the bonds to the other oxygens [ $\text{Li-O}(1)$  1.919,  $\text{Si-O}(1)$  1.629 Å].

Similar distortions occur in the  $\text{Li}(1)\text{O}_4$  and  $\text{BeO}_4$  tetrahedron pairs. Individual bond distances are  $\text{Li-O}(1)$  1.967,  $\text{Be-O}(1)$  1.660 Å compared with  $\text{Li-O}(2)$  1.950,  $\text{Be-O}(2)$  1.634 Å. It is interesting to compare the  $\text{Li-O}$  distances in  $\text{LiO}_4$  tetrahedra which share a common edge with  $\text{BeO}_4$ ,  $\text{SiO}_4$  ( $\gamma\text{-Li}_2\text{BeSiO}_4$ ) and  $\text{AlO}_4$  ( $\gamma\text{-LiAlO}_2$ ) tetrahedra:

$\text{Li-O}^a$ (Å)	$\text{Li-O}^b$ (Å)	Other tetrahedron	$\Delta(\text{Li-O})$ (Å)
1.967	1.950	$\text{BeO}_4$	0.02
2.06	1.95	$\text{AlO}_4^c$	0.11
2.08	1.93	$\text{AlO}_4^d$	0.15
2.092	1.919	$\text{SiO}_4$	0.17

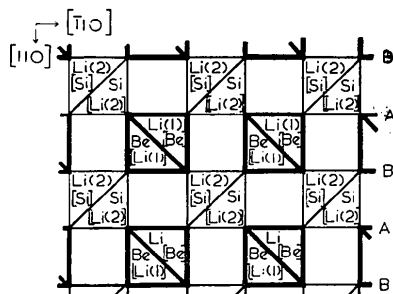


Fig. 2. Idealized (001) projection of  $\gamma\text{-Li}_2\text{BeSiO}_4$ . Straight lines represent  $\text{O-O}$  tetrahedron edges.  $A, B$  refer to layers of oxygen atoms in approximately hexagonal close packing.  $\text{Li}(2)$  etc. refers to a  $\text{Li}(2)$ -centred tetrahedron of oxygen atoms. Shared edges of  $\text{Li}(2)\text{-Si}$  and  $\text{Li}(1)\text{-Be}$  tetrahedron pairs are parallel to  $\mathbf{a}$  and  $\mathbf{b}$  respectively. Atom heights are:  $\text{Li}(2)$ ,  $\text{Si} = \frac{1}{4}$ ;  $\text{Li}(1)$ ,  $\text{Be} = \frac{1}{2}$ ;  $[\text{Li}(2)]$ ,  $[\text{Si}] = \frac{3}{4}$ ;  $[\text{Li}(1)]$ ,  $[\text{Be}] = 0$ .

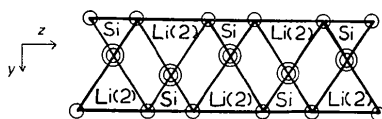


Fig. 3. Idealized (100) projection of an  $\text{Li}(2)\text{O}_4\text{-SiO}_4$  double chain. Open circles represent oxygen atoms; straight lines are  $\text{O-O}$  tetrahedron edges. The two oxygens of each shared edge have slightly different  $c$  values: this has been ignored.

(a) Oxygens of the shared edge; (b) other oxygens; (c) Marezio (1965), single-crystal X-ray diffraction analysis; (d) Bertaut *et al.* (1965), powder neutron-diffraction analysis. The size, and distortion, of the  $\text{LiO}_4$  tetrahedron is similar in all these structures. However, the lithium atom is displaced progressively further from the centre of its tetrahedron and away from the common edge, as the cation in the other tetrahedron changes from  $\text{Be}$  to  $\text{Al}$  to  $\text{Si}$ .

We are grateful to B. G. Cooksley for recording the intensity data. Some of the single-crystal X-ray photographs were provided by F. P. Glasser. Thanks are due to the Computing Centre of the University of Aberdeen for making computing facilities available to us.

## References

- BERTAUT, E. F., DELAPALME, A., BASSI, G., DURIF-VARAMBON, A. & JOUBERT, J. C. (1965). *Bull. Soc. Fr. Minér. Crist.* **88**, 103-108.
- International Tables for X-ray Crystallography* (1968). Vol. III, 2nd ed., pp. 202-203. Birmingham: Kynoch Press.
- MAREZIO, M. (1965). *Acta Cryst.* **19**, 396-400.
- PARTHÉ, E. (1964). *Crystal Chemistry of Tetrahedral Structures*. London and New York: Gordon and Breach.